

## Supporting Information for

# Magnetism in Olivine-type $\text{LiCo}_{1-x}\text{Fe}_x\text{PO}_4$ Cathode Materials: Bridging Theory and Experiment

Vijay Singh,<sup>§</sup> Yelena Gershinsky,<sup>§</sup> Monica Kosa, Mudit Dixit, David Zitoun,\* Dan Thomas Major\*

*Department of Chemistry and the Lise Meitner-Minerva Center of Computational Quantum Chemistry and the Institute for Nanotechnology and Advanced Materials, Bar-Ilan University, Ramat-Gan 52900, Israel*

<sup>§</sup> Equal contribution

\* Electronic mail: [majort@biu.ac.il](mailto:majort@biu.ac.il), [david.zitoun@biu.ac.il](mailto:david.zitoun@biu.ac.il)

**Figure S1:** HRSEM of synthesized (a, b) LiCoPO<sub>4</sub> and (c, d) LiFePO<sub>4</sub>

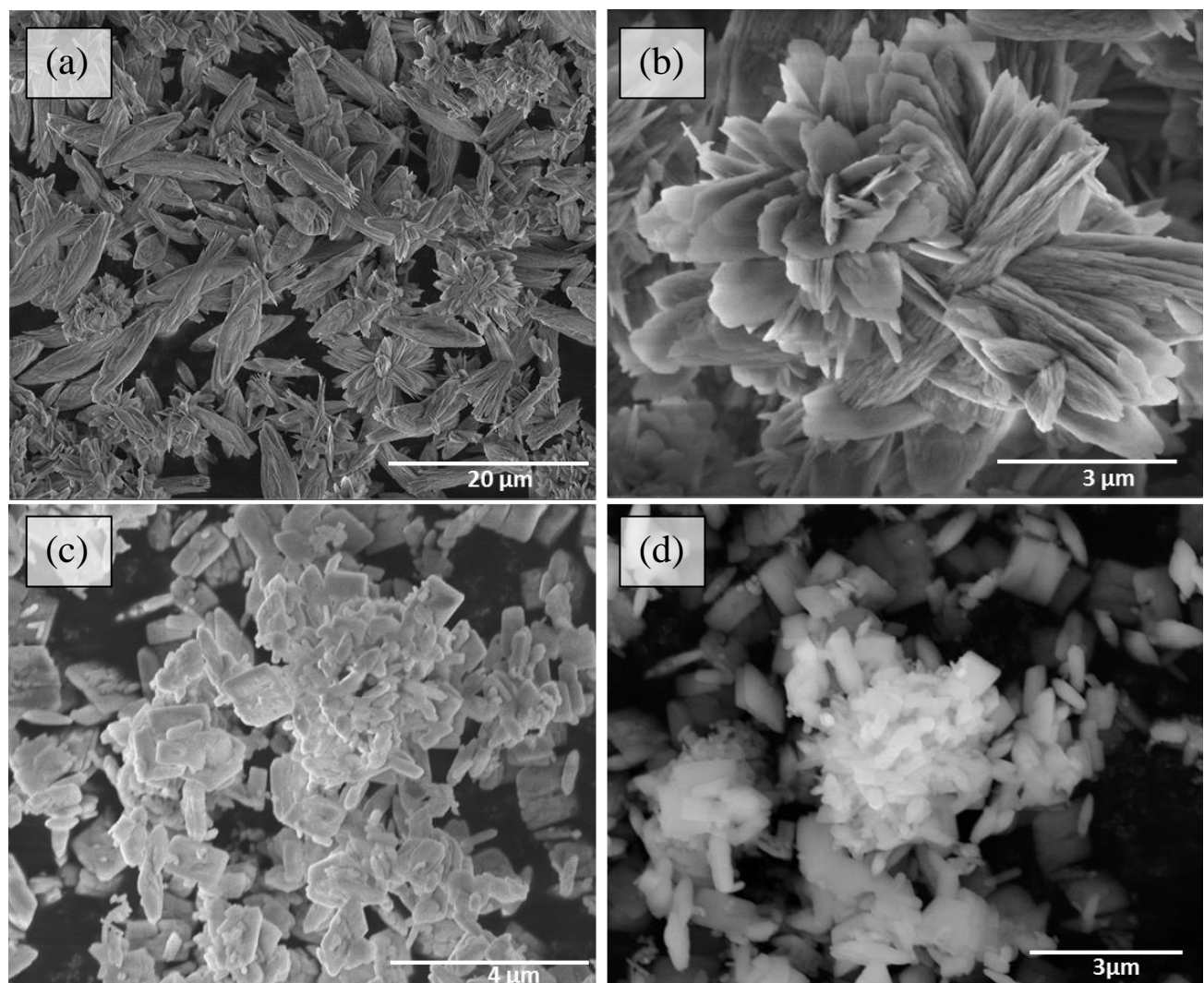


**Figure S2.** Rietveld refinement for the  $\text{LiCo}_{1-x}\text{Fe}_x\text{PO}_4$  solid solutions.

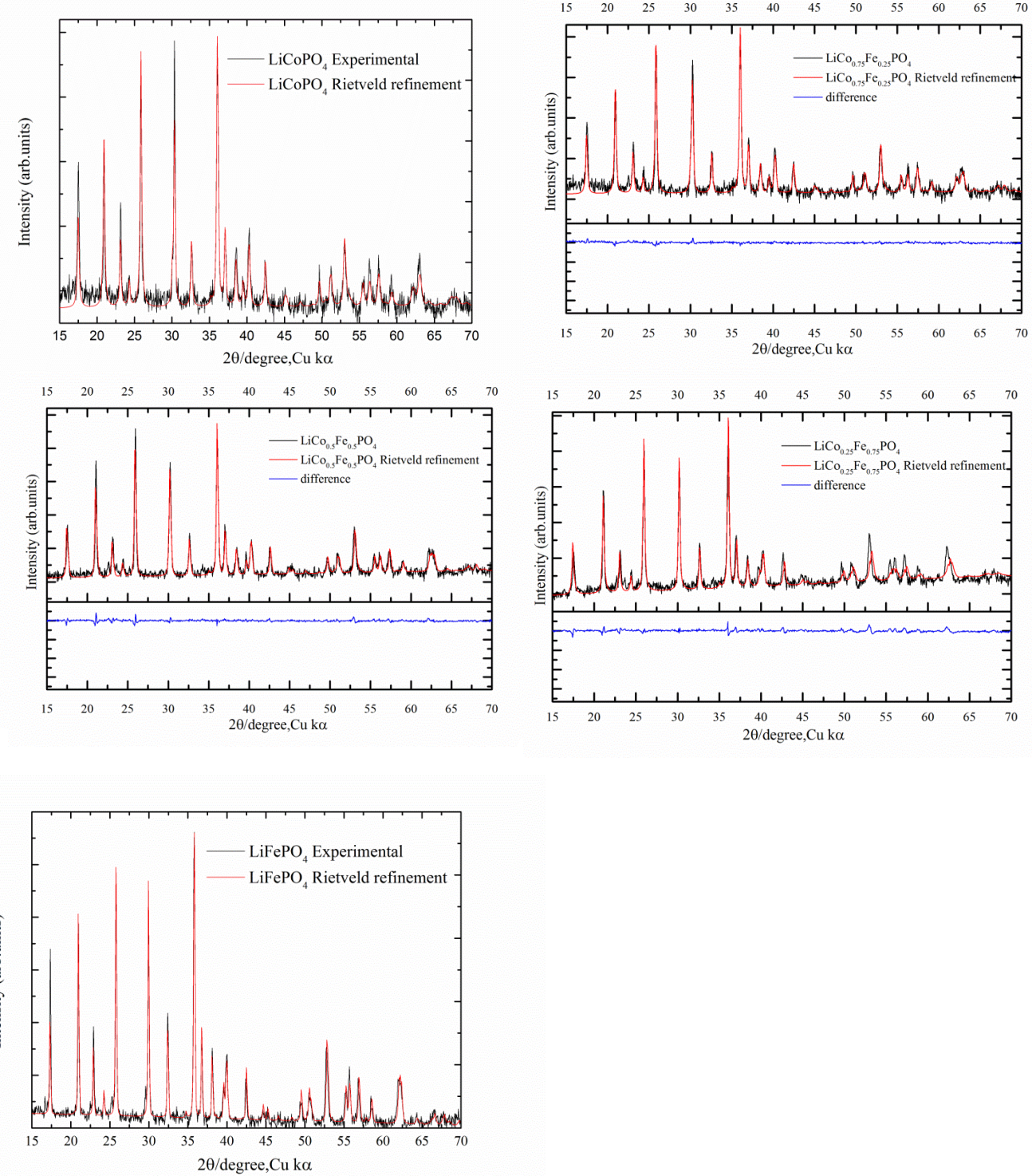


**Figure S3.** Model unit cells employed for all calculations, where (a, e) are the four formula unit cell for the pure olivines, LCP (i.e.  $x = 0.00$ ) and LFP (i.e.  $x = 1.00$ ), respectively, and (b, c, and d) are the eight formula unit cell systems used for  $x = 0.25$ ,  $0.50$ , and  $0.75$ , respectively.

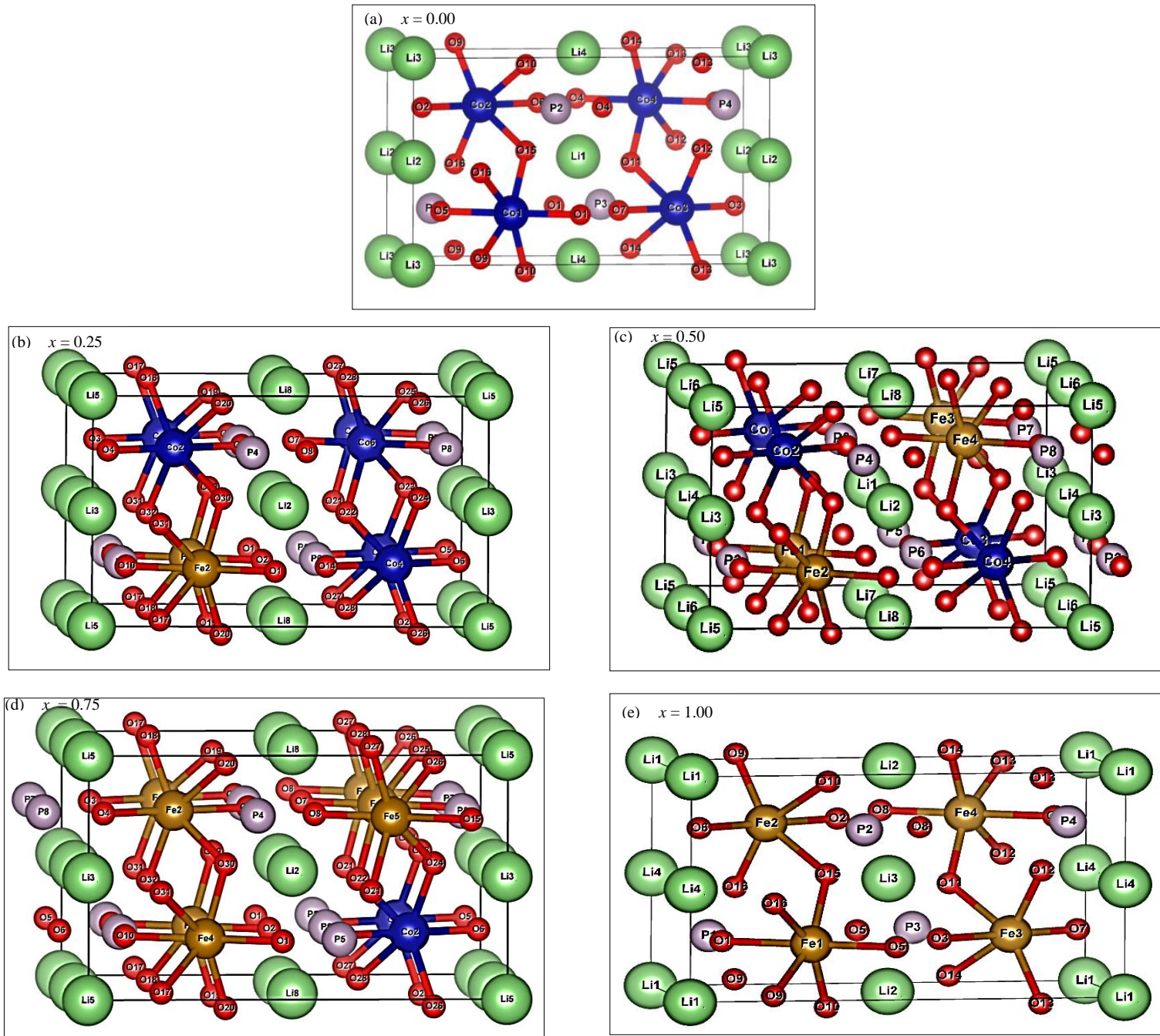


**Figure S4** Calculated LSDA + U + SOC canting angle for LCP and LFP as a function of  $X$  for  $U = 6.7$  eV and 5.3 eV, respectively. The experimental value for the canting angle is equal to  $4.6^\circ$  for LCP and is denoted by a dotted straight line.<sup>1</sup>

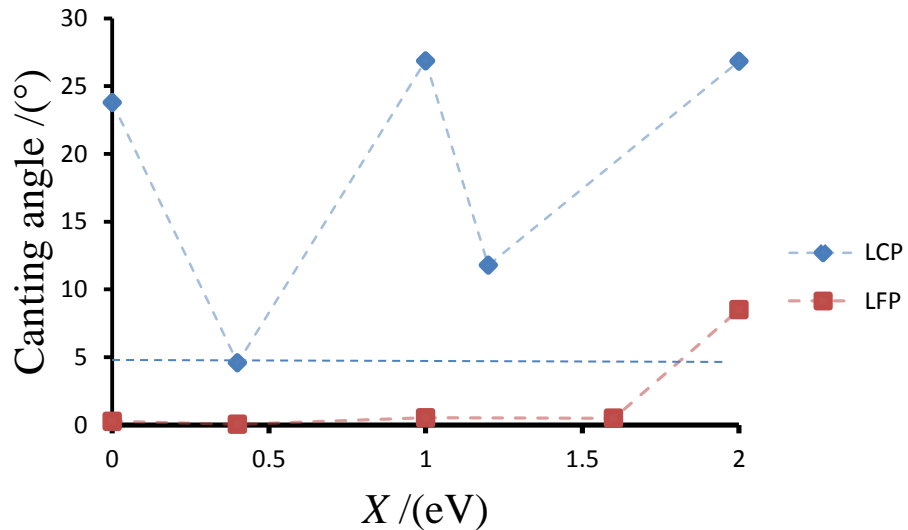


**Figure S5.** Relative energies per formula unit cell for  $\text{LiCo}_{1-x}\text{Fe}_x\text{PO}_4$  ( $x = 0.00, 0.25, 0.50, 0.75$ , and  $1.00$ ) systems, along different spin quantization axes.

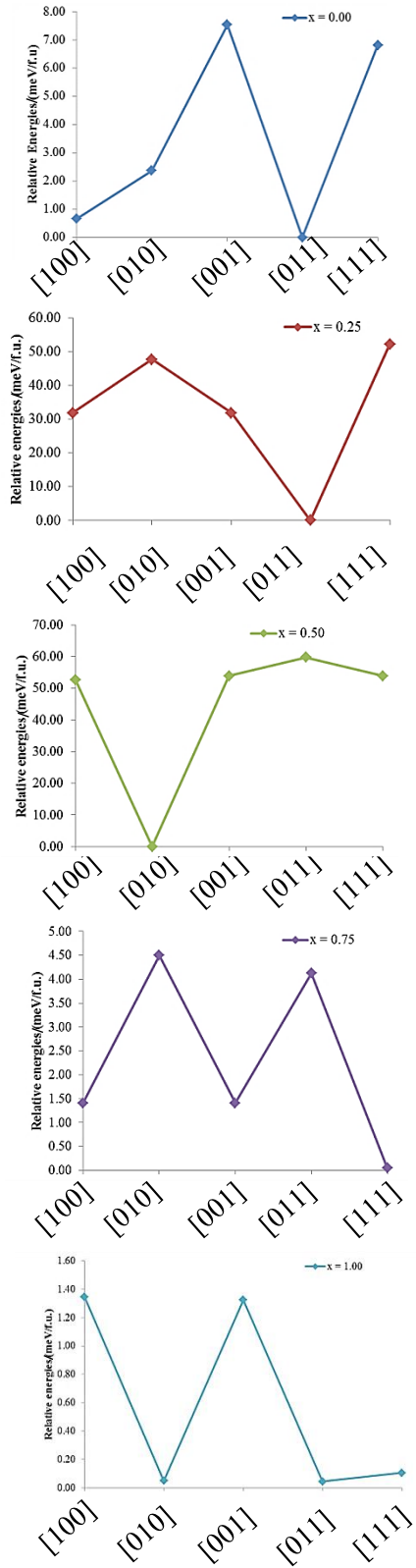


**Figure S6.** Comparison of the total density of states for the pure LCP olivine along two sets of spin magnetization axis: [101] and [011].

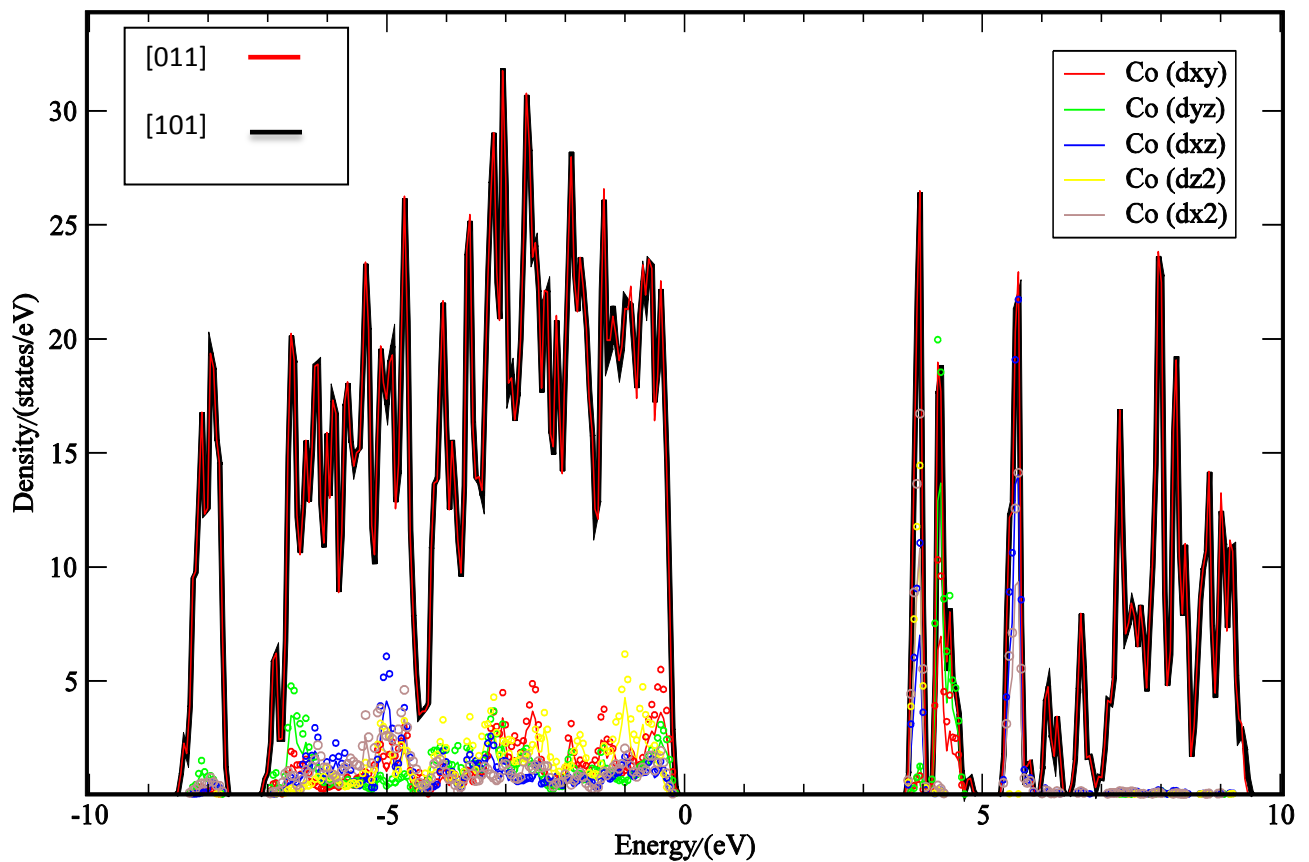


**Figure S7.** Computed orbital projected density of states for the Fe- $3d_{3z-2}$  orbital for the  $\text{LiCo}_{1-x}\text{Fe}_x\text{PO}_4$  ( $x = 0.25, 0.50, 0.75$ , and  $1.00$ ) systems.

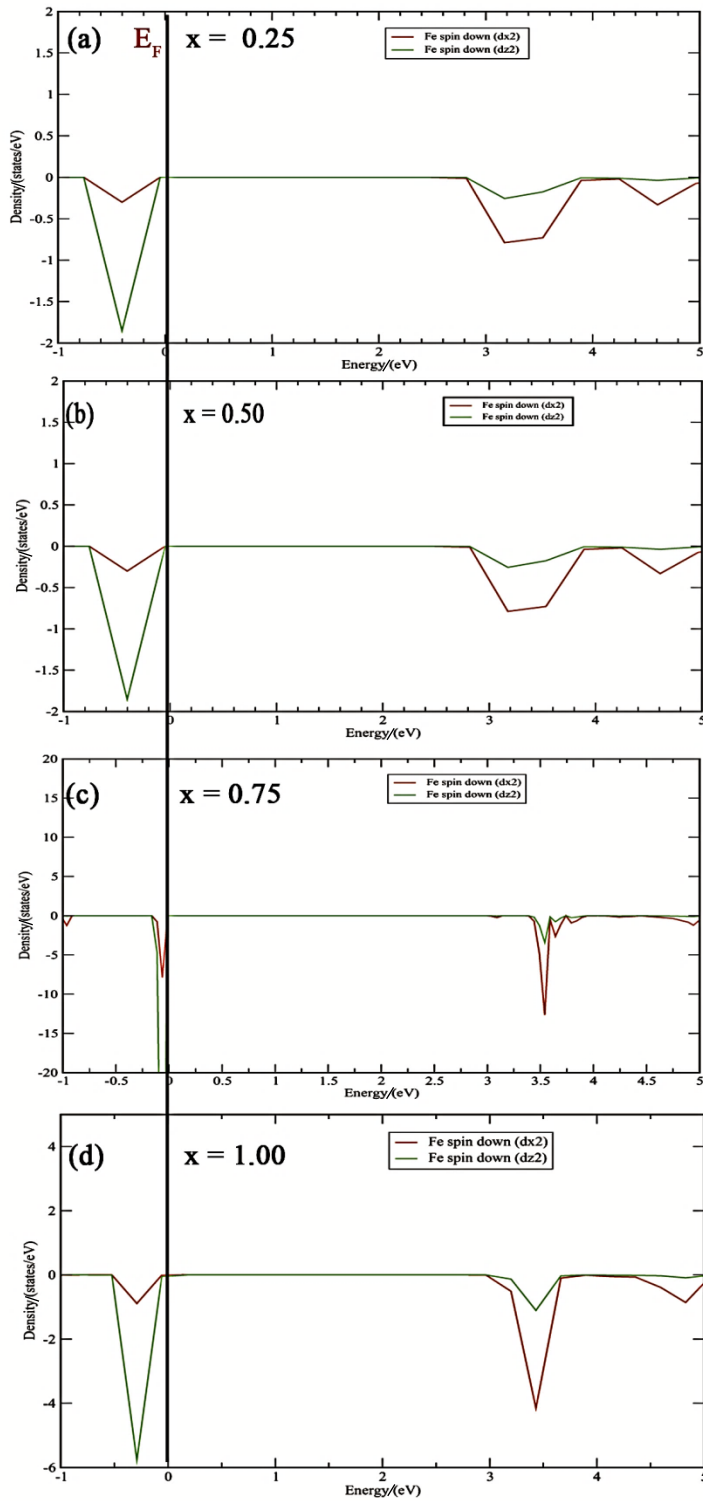


**Figure S8.** The charge density corresponding to the HOMO level for  $\text{LiCo}_{1-x}\text{Fe}_x\text{PO}_4$  ( $x = 0.25, 0.50, 0.75$ , and  $1.00$ ).

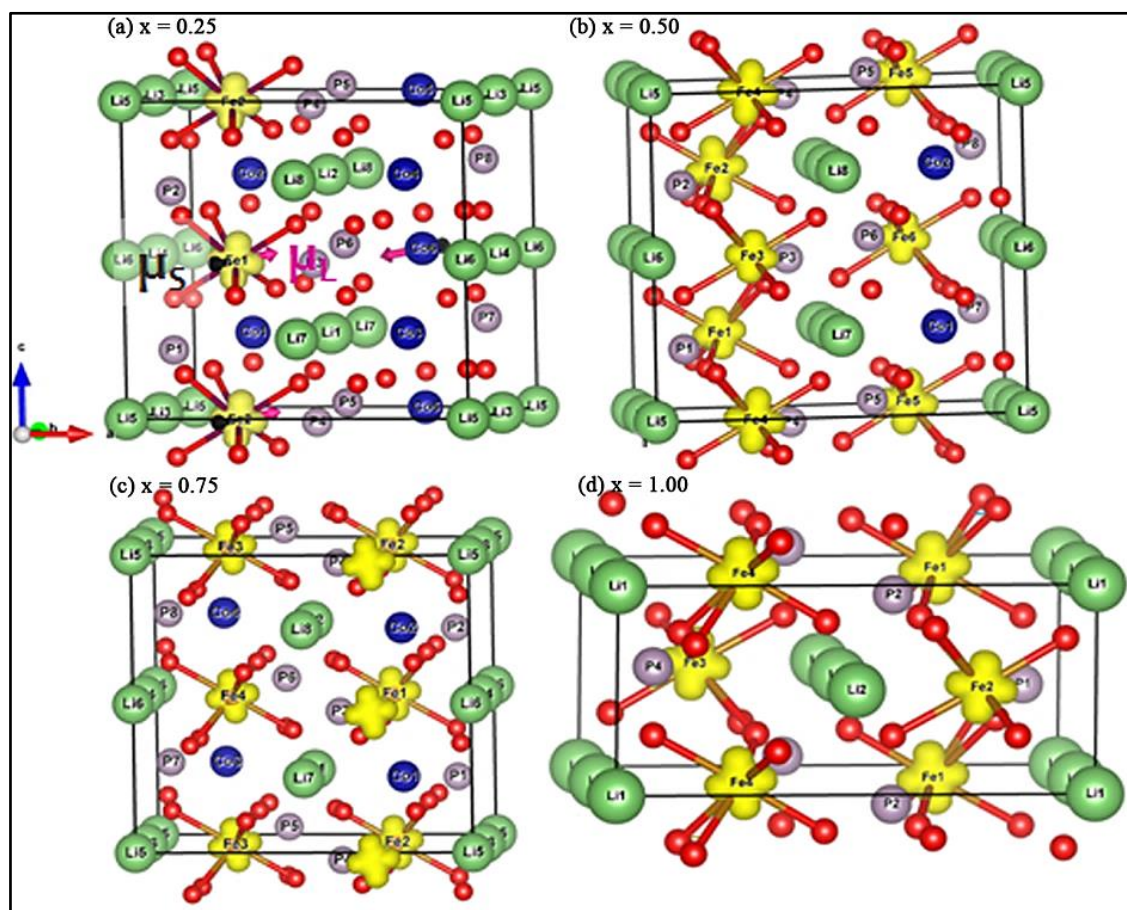


**Figure S9.** Total and atom projected density of states for  $\text{LiCo}_{1-x}\text{Fe}_x\text{PO}_4$  ( $x = 0.00, 0.25, 0.50, 0.75$ , and  $1.00$ ).

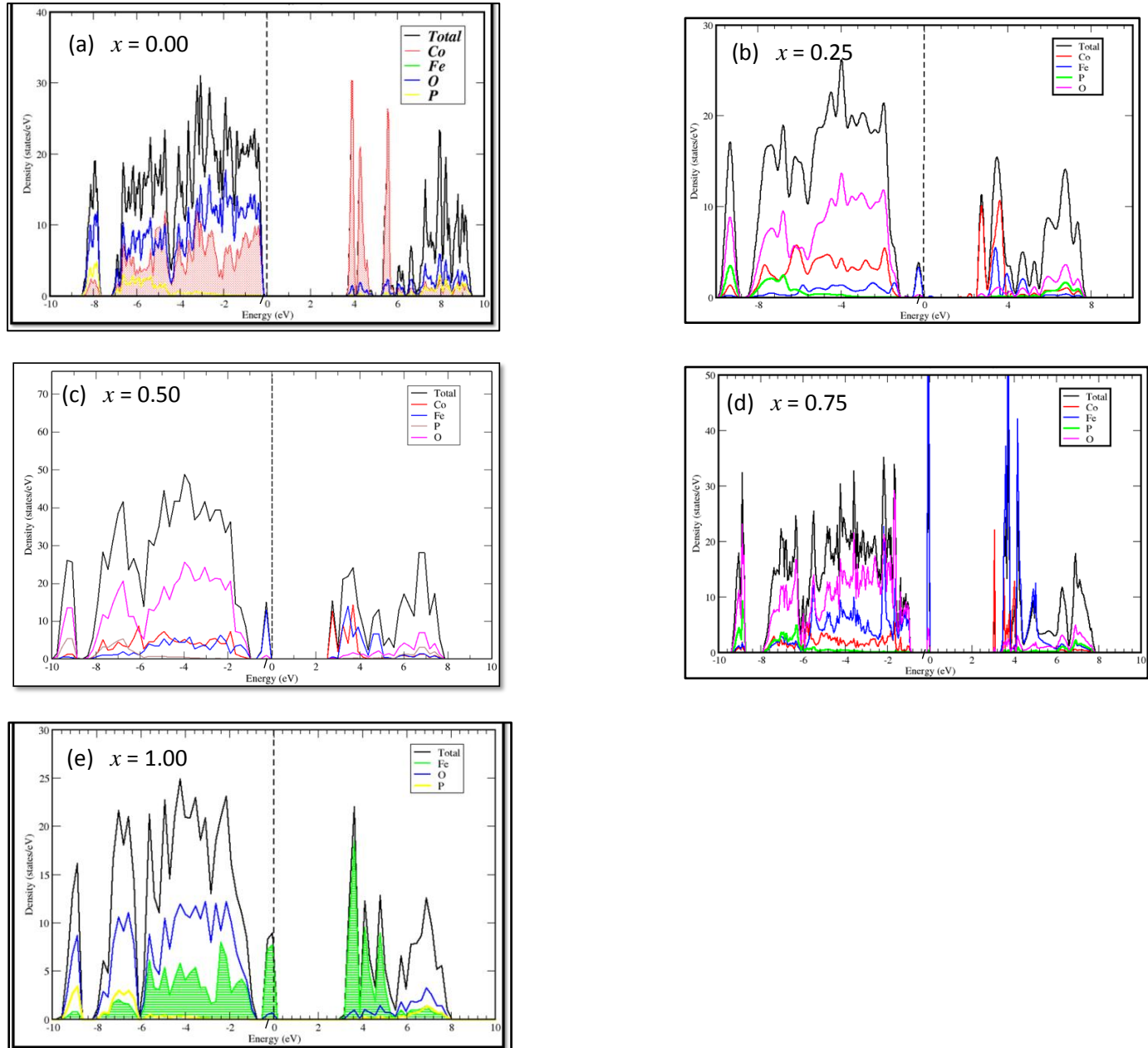
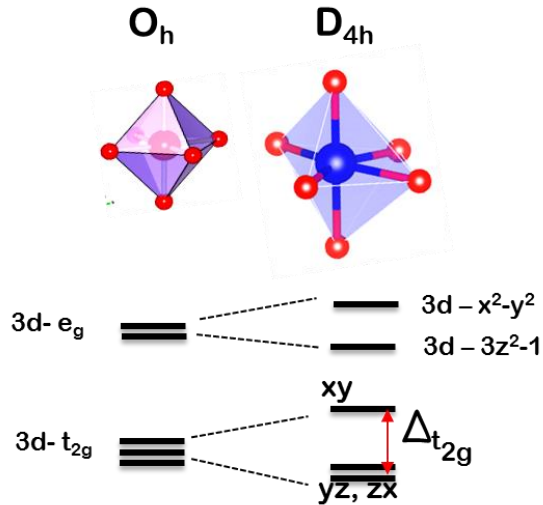


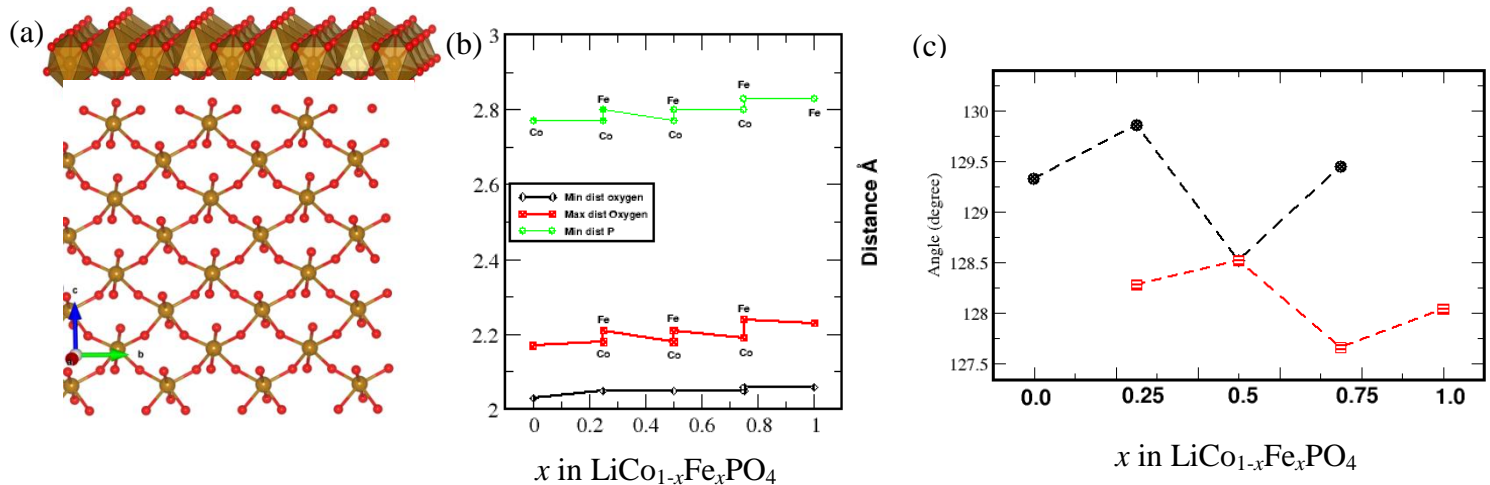
**Figure S10.** Schematic depiction of the splitting of the 3d-t<sub>2g</sub> orbitals in a cubic (O<sub>h</sub>) to tetragonal (D<sub>4h</sub>) symmetry transformation.



In an ideal octahedral arrangement (i.e. a cubic symmetric crystal field), Co<sup>+</sup> and Fe<sup>+</sup> ions do not exhibit orbital magnetic moments. Okamoto et al. have demonstrated that the tetragonal crystal field splits the three fold degenerate (t<sub>2g</sub>) levels into a two fold degenerate level (xz and yz orbitals) and a non-degenerate level (xy orbital).<sup>2</sup> If the splitting energy is larger than the strength of the spin-orbit coupling (i.e. Δt<sub>2g</sub>>> λ), the ground state will approach |xy>. This leads to complete quenching of the orbital angular momentum (*L*=0) for the transition metals. If the tetragonal crystal field splitting is smaller than that of spin-orbit coupling (Δt<sub>2g</sub><< λ), then the t<sub>2g</sub> orbitals will mix. As a result, the ground state is written as the following linear combination,  $1/\sqrt{3}(|xy\rangle + |yz\rangle + i|zx\rangle)$ , with a concomitant large orbital angular momentum.<sup>3, 4</sup> Therefore, a system might gain considerable orbital moment during the transformation from a cubic (O<sub>h</sub>) to a tetragonal (D<sub>4h</sub>) symmetry. In tetragonal symmetry, the computed M - O distances for all compositions reveal considerable anisotropy (where two short and two long in plane distances and one short and one long out of plane distances exist). This is in agreement with our previous results, where bond distances suggest the lack of cubic ligand symmetry of the transition metals.<sup>5</sup> A schematic representation of the electronic

structure for the  $t_{2g}$  orbital in the presence of cubic and tetragonal environment, was provided above.

**Figure S11.** Mechanism 1: (a) A magnetic layer of olivines, which is also a bc-plane of the unit cell containing Metal-Oxygen-Metal networks, where brown spheres represent metal ions, and red spheres represent oxygen atoms, (b) the change in bond distances between Co-O, Fe-O, Co-P, and Fe-P, and (c) the change in bond angles between Co-O-Co and Fe-O-Fe as a function of  $x$  in  $\text{LiCo}_{1-x}\text{Fe}_x\text{PO}_4$  ( $x = 0.00, 0.25, 0.50, 0.75$ , and  $1.00$ ).

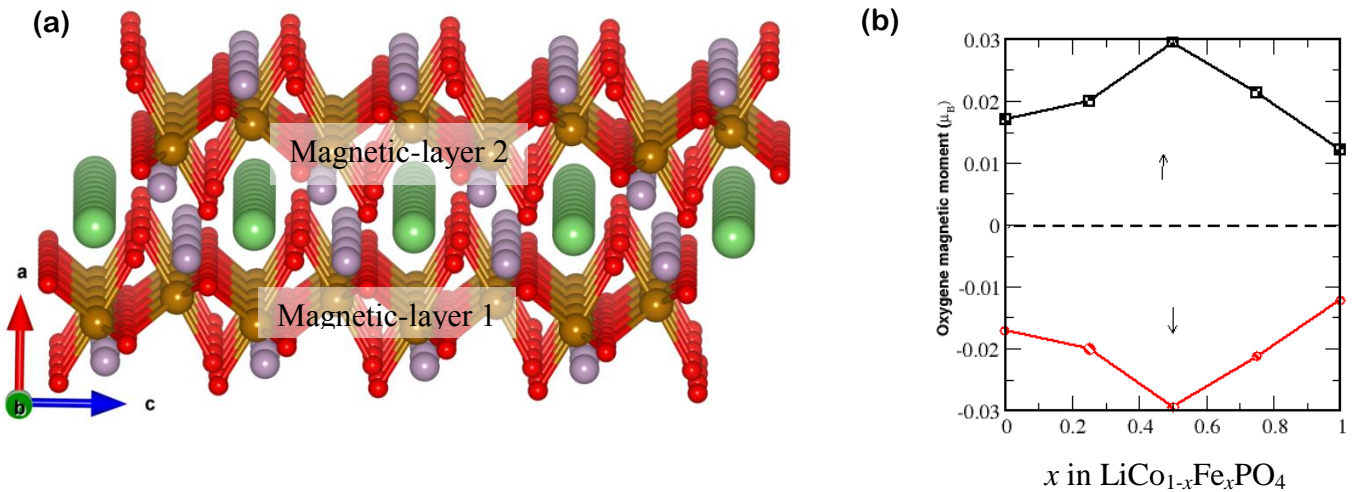


In the studied olivines materials, octahedrally coordinated oxygen atoms surround each magnetic ion in the transition metal layer and these octahedra are connected with corner-shared oxygen. These represent the ideal structure, where the GKA rule is applicable. It is clear from the structure (refer Figure S11a) that the magnetic layers (in the bc-plane) are connected through oxygen atoms, and form extensive M – O – M networks. The reduced AFM stability is likely due to the smaller M – O – M bond angle, which may lead to weakening of the GKA super exchange.<sup>6</sup> The computed bond-distance between M – O (M = Fe,Co), and bond angle between M – O – M for the relaxed unit cell is shown in Figure S11(b, c). We observe an increasing trend with  $x$ , in the Fe-O and Co-O bond lengths. This is in the agreement with the findings of Kosava et al.<sup>7</sup>

In contrast, we found slight fluctuation of the bond-angles for Fe – O – Fe, as well as for the Co – O - Co bond angles as a function of  $x$  (Figure S9c). Moreover, the bond-angle Fe – O –

Fe is smaller than the Co – O – Co bond angle. Also, it is important to note that the presence of values between  $90^\circ$  and  $180^\circ$  for the M – O – M bond angle; such values do not allow us to rationalize our results within the Goonenough - Kanamori superexchange model completely. Therefore, it is hard to make any conclusion for rising trends in Néel temperature at this moment based on this model.

**Figure S12.** Mechanism 2: Two magnetic layers of olivines separated by non-magnetic Li and P ions (a), and the change in the computed polarization of an oxygen ion (i.e. oxygen magnetic moment) as a function of  $x$  in  $\text{LiCo}_{1-x}\text{Fe}_x\text{PO}_4$  ( $x = 0.00, 0.25, 0.50, 0.75$ , and  $1.00$ ).



### Mechanism 2: M – O – O – M:

Surprisingly, Out of plane FM interactions are shown to be substantial in pure olivines, for instance, in LCP with values of  $J^{Exp\perp} = -0.163 \text{ meV}^8$  and for the LFP values of  $J^{Exp\perp} = 0.021 \text{ meV}^9$  and  $J^{Theory\perp} = -0.92 \text{ meV}^{10}$ . In the following, we shall explore all potential paths which offer a possible of out of plane exchange interaction.

As shown in Figure S12, between the two magnetic layers, there is a non-magnetic layer of P and Li ions. However, a dipole-mediated interaction of the type M – O – O – M between the two metal ions, which are part of an octahedra lying in different magnetic layers in the bc plane, is possible. Considerable magnetic moments on the oxygen atoms can facilitate such dipolar interactions. In the view of the above, we have calculated the polarization of the oxygen (s+p) electrons, and surprisingly a decreasing trend in the polarization of oxygen after  $x = 0.50$  is observed (Figure S12). The lack of a linear trend rules out in plane (M – O - M), as well as out of plane (M – O – O - M) interactions, and thus the rising trend in the Néel temperature cannot be explained by these types of exchange coupling. Therefore, in the main

manuscript, we have explored the remaining possibility of an interaction path of the type M-O-P-O-M in detail. We conclude that out of plane exchange interaction between two magnetic ions is mediated through this latter exchange path.

**Figure S13.** The pd $\pi$  - antibonding orbitals obtained by mixing Fe-3d<sub>3z-2</sub><sup>2</sup> and O<sub>p<sub>x</sub>/p<sub>y</sub></sub> orbitals are clearly observed for all the six oxygens surrounding the Fe ions for mixed olivines  $x = 0.25$ .

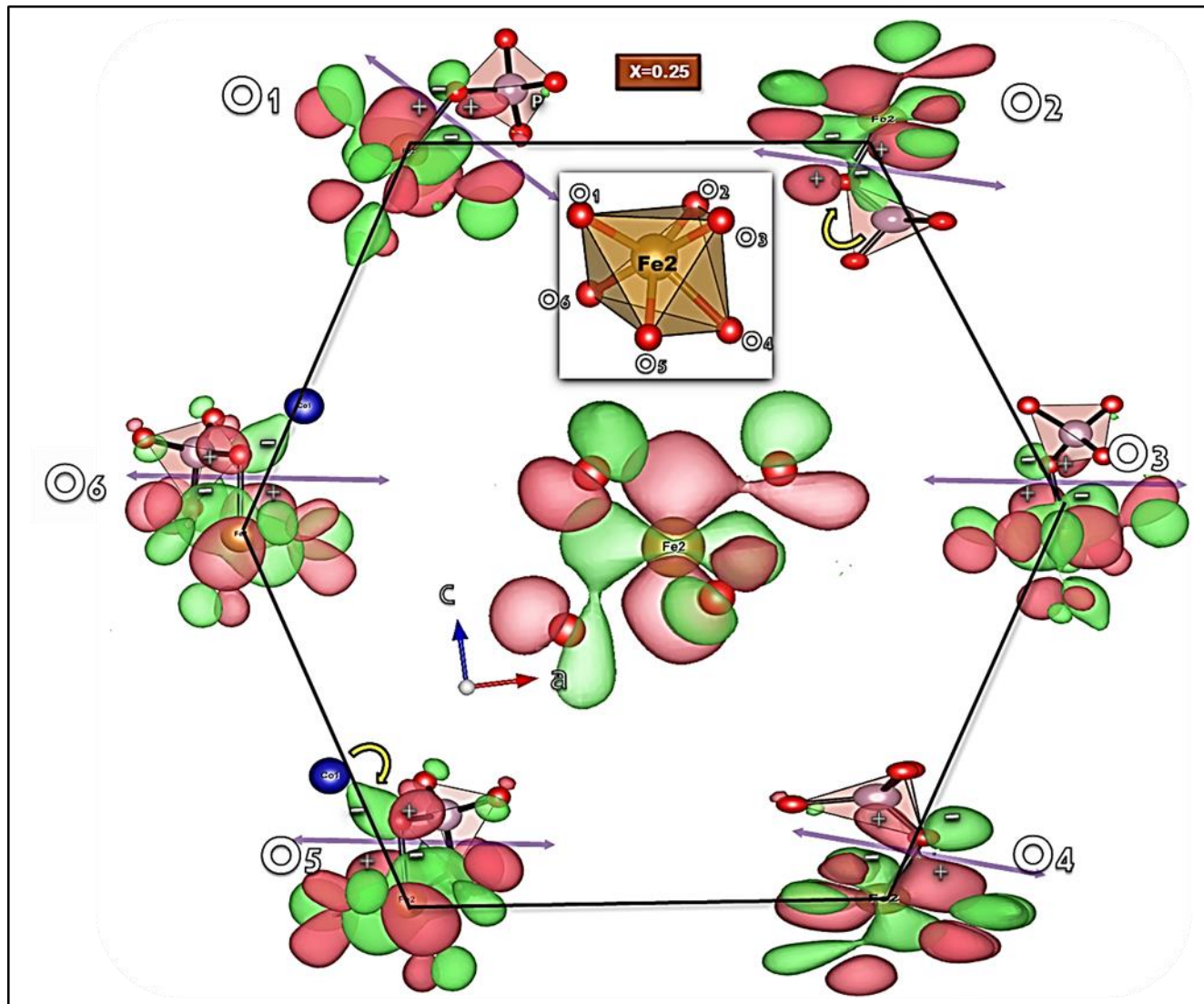


**Figure S14.** The pd $\pi$  - antibonding orbitals obtained by mixing Fe-3d<sub>3z-2</sub><sup>2</sup> and O<sub>p<sub>x</sub>/p<sub>y</sub></sub> orbitals are clearly observed for all the six oxygens surrounding the Fe ions for pure olivines  $x = 1.00$ .

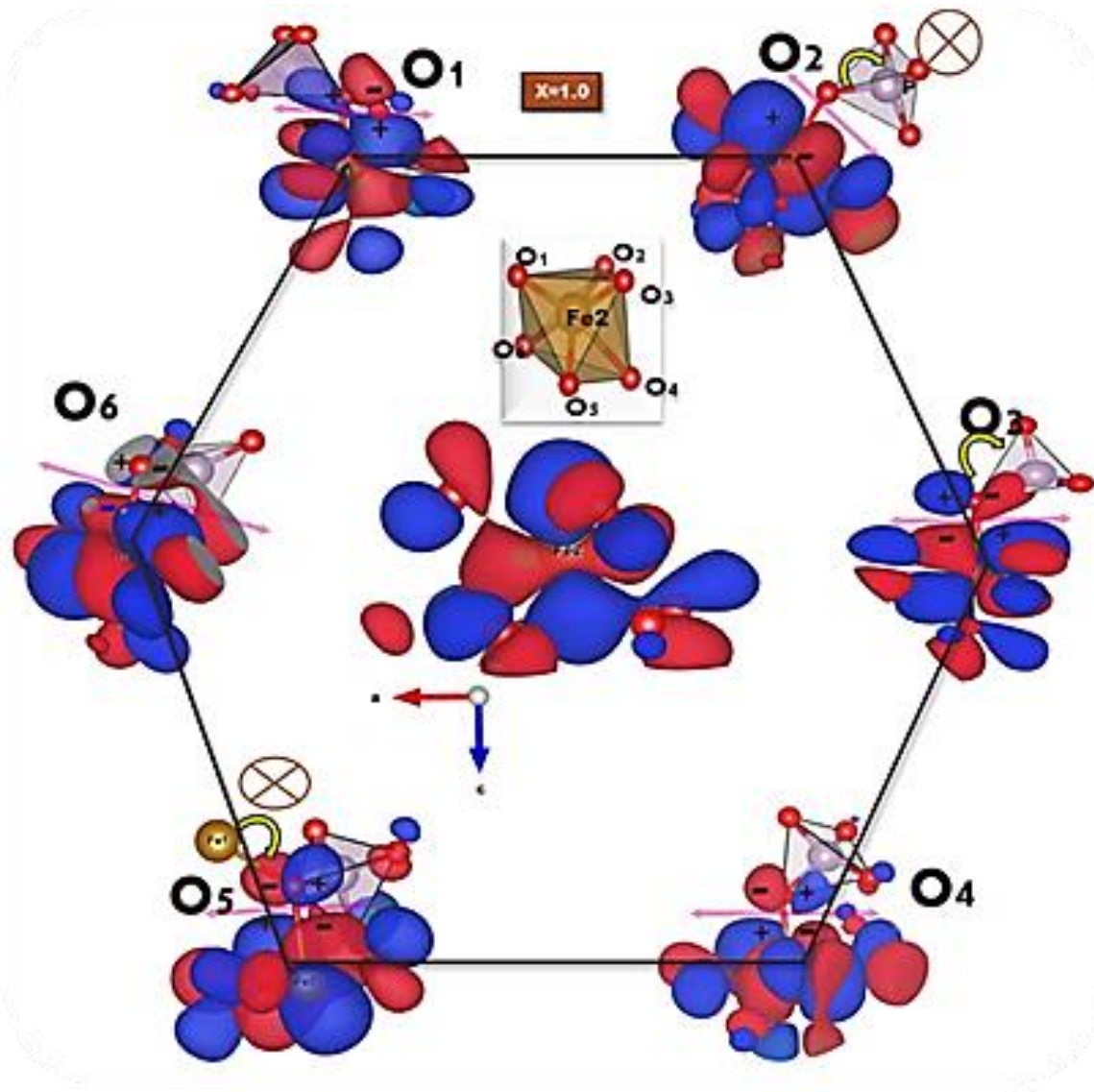


**Figure S15.** Fe  $3d_{3z}^{2-2}$  Wannier function for the mixed composites  $x = 0.50$  and  $0.75$ .

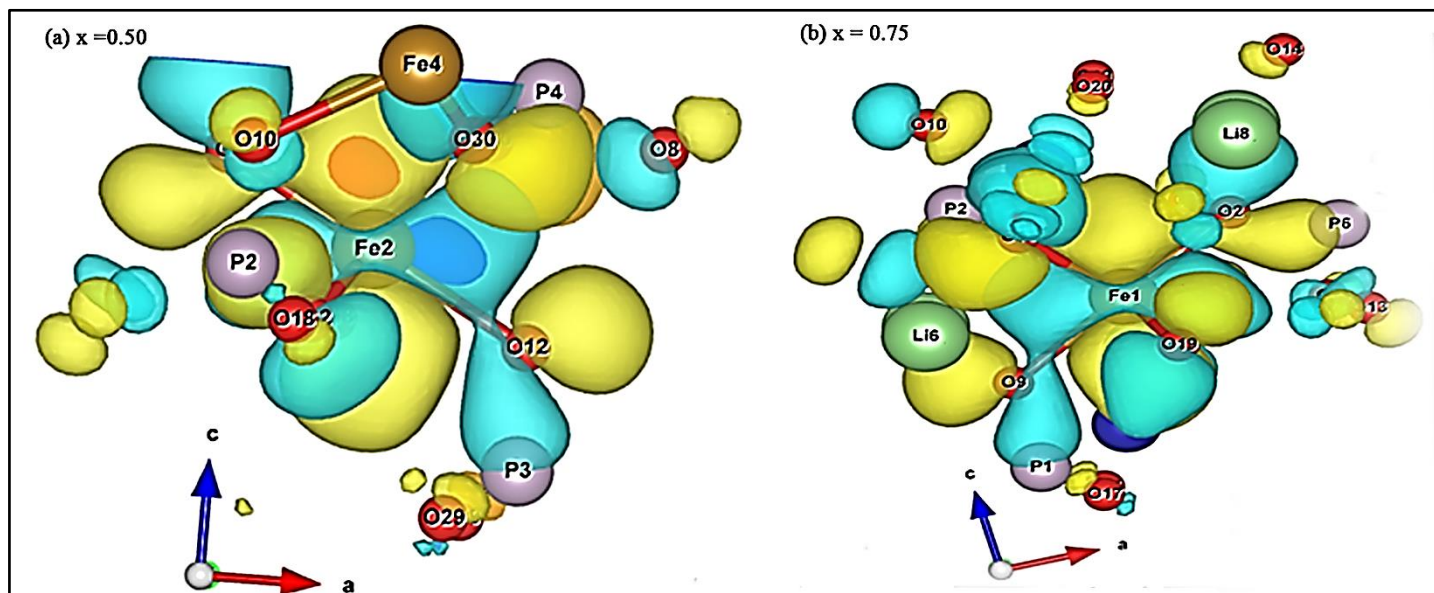


**Table S1.** Synthesized LiCoPO<sub>4</sub>, LiFePO<sub>4</sub> and their solid solutions LiCo<sub>1-x</sub>Fe<sub>x</sub>PO<sub>4</sub>.

		Li /(%wt)	Co /(%wt)	P/ (%wt)	Fe /(%wt)
LiCoPO <sub>4</sub>	Experimental	29.79%	31.74%	38.47%	
	Calculated	33.34%	33.38%	33.28%	
LiCo <sub>0.75</sub> Fe <sub>0.25</sub> PO <sub>4</sub>	Experimental	36.44%	24.32%	33.01%	6.23%
	Calculated	33.61%	24.83%	33.21%	8.35%
LiCo <sub>0.5</sub> Fe <sub>0.5</sub> PO <sub>4</sub>	Experimental	36.62%	15.99%	33.17%	14.22%
	Calculated	33.46%	16.70%	33.21%	16.63%
LiCo <sub>0.25</sub> Fe <sub>0.75</sub> PO <sub>4</sub>	Experimental	36.42%	7.51%	35.71%	20.37%
	Calculated	33.26%	8.39%	33.36%	24.99%
LiFePO <sub>4</sub>	Experimental	33.28%		36.27%	30.45%
	Calculated	33.74%		33.12%	33.14%

**Table S2.** Experimental/Computed (from first principles DFT) cell parameters ( $\text{\AA}$ ) used in the simulation of  $\text{LiCo}_{1-x}\text{Fe}_x\text{PO}_4$  obtained by Rietveld refinement.

	$\text{LiFePO}_4$	$\text{LiCoPO}_4$	$\text{LiCo}_{0.25}\text{Fe}_{0.75}\text{PO}_4$	$\text{LiCo}_{0.5}\text{Fe}_{0.5}\text{PO}_4$	$\text{LiCo}_{0.75}\text{Fe}_{0.25}\text{PO}_4$
$a / (\text{\AA})$	10.3070(8)/10.281	10.198(4)/10.211	10.2248(19)/10.185	10.2338(16)/10.224	10.218(4)/10.246
$b / (\text{\AA})$	5.9863(6)/6.002	5.911(2)/5.856	5.9339(9)/5.937	5.9417(9)/5.958	5.928(2)/5.979
$c / (\text{\AA})$	4.6787(5)/4.695	4.694(2)/4.6900	4.6466(8)/4.6902	4.6756(8)/4.6956	4.6913(18)/4.698
$V / (\text{\AA}^3)$	288.68(5)/289.71	282.93(19)/280.47	281.92(8)/283.61	284.31(8)/285.99	284.19(18)/287.71
Rwp	3.00%	2.60%	3.41%	2.63%	2.87%
S	1.9898	2.4769	2.5181	2.1220	2.4765

**Table S3.** All the relaxed atomic coordinates used in the simulation of LiCoPO<sub>4</sub>.

	x	y	z
Li	0.5000	0.5000	0.5000
Li	0.0000	0.5000	0.0000
Li	0.0000	0.0000	0.0000
Li	0.5000	0.0000	0.5000
Co	0.2766	0.2500	0.9851
Co	0.2234	0.7500	0.4851
Co	0.7766	0.2500	0.5149
Co	0.7234	0.7500	0.0149
P	0.0941	0.2500	0.4233
P	0.4059	0.7500	0.9233
P	0.5941	0.2500	0.0767
P	0.9059	0.7500	0.5767
O	0.4548	0.2500	0.2051
O	0.0452	0.7500	0.7051
O	0.9548	0.2500	0.2949
O	0.5452	0.7500	0.7949
O	0.0960	0.2500	0.7493
O	0.4040	0.7500	0.2493
O	0.5960	0.2500	0.7507
O	0.9040	0.7500	0.2507
O	0.1686	0.0420	0.2863
O	0.3314	0.9580	0.7862
O	0.6686	0.4580	0.2138
O	0.8314	0.5420	0.7137
O	0.8314	0.9580	0.7138
O	0.6686	0.0420	0.2137
O	0.3314	0.5420	0.7863
O	0.1686	0.4580	0.2862

**Table S4.** All the relaxed atomic coordinates used in the simulation of LiCo<sub>0.75</sub>Fe<sub>0.25</sub>PO<sub>4</sub>.

	x	y	z
Li	0.501861	0.499262	0.250844
Li	0.501849	0.499263	0.750844
Li	-0.00085	0.499382	0.999858
Li	-0.00085	0.499385	0.499857
Li	-0.00084	0.000599	0.999857
Li	-0.00085	0.000602	0.499857
Li	0.501831	0.000766	0.250844
Li	0.501843	0.000766	0.750844
Co	0.22259	0.749992	0.243932
Co	0.22259	0.749998	0.74393
Co	0.777323	0.249997	0.26105
Co	0.777324	0.249995	0.761049
Co	0.723259	0.750002	0.007845
Co	0.723259	0.750006	0.507844
Fe	0.277629	0.250003	0.488078
Fe	0.277629	0.250003	0.988077
P	0.091456	0.24999	0.207892
P	0.091457	0.249987	0.707889
P	0.405689	0.750005	0.46083
P	0.40569	0.750006	0.960826
P	0.596602	0.250003	0.041512
P	0.596601	0.250011	0.541515
P	0.906838	0.749996	0.289069
P	0.906838	0.749996	0.789067
O	0.45546	0.249987	0.10363
O	0.455463	0.250005	0.603632
O	0.048223	0.749997	0.351129
O	0.048223	0.749998	0.851129
O	0.949879	0.250002	0.14711
O	0.94988	0.249985	0.64711
O	0.547177	0.750006	0.399911
O	0.547176	0.750023	0.899906
O	0.094316	0.249994	0.371066
O	0.09432	0.249971	0.871066
O	0.401	0.750007	0.124162
O	0.401001	0.750001	0.624162
O	0.599577	0.250016	0.378072
O	0.59958	0.250011	0.878069
O	0.902063	0.750002	0.12628
O	0.902063	0.749992	0.626282

O	0.162451	0.041952	0.139045
O	0.162462	0.041955	0.639035
O	0.333568	0.955505	0.390938
O	0.333558	0.955506	0.890946
O	0.668551	0.457444	0.109608
O	0.668559	0.457438	0.609601
O	0.834876	0.543812	0.358931
O	0.834878	0.543811	0.858936
O	0.834872	0.956175	0.358937
O	0.834874	0.956171	0.858932
O	0.668571	0.042576	0.109596
O	0.668561	0.042578	0.6096
O	0.333559	0.544505	0.39095
O	0.333569	0.544505	0.890938
O	0.162462	0.458025	0.139035
O	0.162452	0.458032	0.639045

**Table S5.** All the relaxed atomic coordinates used in the simulation of LiCo<sub>0.5</sub>Fe<sub>0.5</sub>PO<sub>4</sub>.

	x	y	z
Li	0.4997	0.4999	0.2499
Li	0.4997	0.4999	0.7499
Li	0.0001	0.5000	1.0000
Li	0.0001	0.5000	0.5000
Li	0.0000	0.0000	1.0000
Li	0.0000	0.0000	0.5000
Li	0.4997	0.0001	0.2499
Li	0.4997	0.0001	0.7499
Co	0.2220	0.7500	0.2386
Co	0.2220	0.7500	0.7386
Co	0.7780	0.2500	0.2615
Co	0.7780	0.2500	0.7615
Fe	0.2772	0.2500	0.4887
Fe	0.2772	0.2500	0.9887
Fe	0.7228	0.7500	0.0113
Fe	0.7228	0.7500	0.5113
P	0.0914	0.2500	0.2107
P	0.0914	0.2500	0.7107
P	0.4047	0.7500	0.4593
P	0.4047	0.7500	0.9593
P	0.5954	0.2500	0.0407
P	0.5954	0.2500	0.5407
P	0.9087	0.7500	0.2893
P	0.9087	0.7500	0.7893
O	0.4550	0.2500	0.1027
O	0.4550	0.2500	0.6027
O	0.0488	0.7500	0.3517
O	0.0488	0.7500	0.8517
O	0.9513	0.2500	0.1484
O	0.9513	0.2500	0.6484
O	0.5450	0.7500	0.3972
O	0.5450	0.7500	0.8972
O	0.0938	0.2500	0.3741
O	0.0938	0.2500	0.8741
O	0.4004	0.7500	0.1229
O	0.4004	0.7500	0.6229
O	0.5995	0.2500	0.3771
O	0.5995	0.2500	0.8771
O	0.9063	0.7500	0.1259
O	0.9063	0.7500	0.6259

O	0.1636	0.0436	0.1429
O	0.1636	0.0436	0.6429
O	0.3326	0.9554	0.3910
O	0.3326	0.9554	0.8910
O	0.6674	0.4554	0.1090
O	0.6674	0.4554	0.6090
O	0.8365	0.5435	0.3571
O	0.8365	0.5435	0.8571
O	0.8365	0.9565	0.3572
O	0.8365	0.9565	0.8572
O	0.6675	0.0446	0.1089
O	0.6675	0.0446	0.6089
O	0.3326	0.5446	0.3910
O	0.3326	0.5446	0.8910
O	0.1636	0.4564	0.1429
O	0.1636	0.4564	0.6429

**Table S6.** All the relaxed atomic coordinates used in the simulation of LiCo<sub>0.25</sub>Fe<sub>0.75</sub>PO<sub>4</sub>.

	x	y	z
Li	0.5021	0.5009	0.2496
Li	0.5021	0.5009	0.7496
Li	-0.0017	0.5009	0.0001
Li	-0.0017	0.5009	0.5001
Li	-0.0017	0.9991	0.0001
Li	-0.0017	0.9991	0.5001
Li	0.5021	0.9991	0.2496
Li	0.5021	0.9991	0.7496
Co	0.7809	0.2500	0.2586
Co	0.7809	0.2500	0.7586
Fe	0.2187	0.7500	0.2380
Fe	0.2187	0.7500	0.7380
Fe	0.2793	0.2500	0.4880
Fe	0.2793	0.2500	0.9880
Fe	0.7207	0.7500	0.0125
Fe	0.7207	0.7500	0.5125
P	0.0923	0.2500	0.2101
P	0.0923	0.2500	0.7101
P	0.4059	0.7500	0.4595
P	0.4059	0.7500	0.9595
P	0.5962	0.2500	0.0397
P	0.5962	0.2500	0.5397
P	0.9046	0.7500	0.2910
P	0.9046	0.7500	0.7910
O	0.4562	0.2500	0.1019
O	0.4562	0.2500	0.6019
O	0.0442	0.7500	0.3549
O	0.0442	0.7500	0.8549
O	0.9526	0.2500	0.1471
O	0.9526	0.2500	0.6471
O	0.5455	0.7500	0.3959
O	0.5455	0.7500	0.8959
O	0.0941	0.2500	0.3732
O	0.0940	0.2500	0.8732
O	0.4044	0.7500	0.1227
O	0.4044	0.7500	0.6227
O	0.6008	0.2500	0.3767
O	0.6008	0.2500	0.8767
O	0.9045	0.7500	0.1278
O	0.9045	0.7500	0.6278

O	0.1646	0.0449	0.1423
O	0.1645	0.0449	0.6423
O	0.3338	0.9554	0.3922
O	0.3338	0.9554	0.8922
O	0.6680	0.4544	0.1090
O	0.6680	0.4544	0.6090
O	0.8329	0.5434	0.3581
O	0.8329	0.5434	0.8580
O	0.8329	0.9566	0.3581
O	0.8329	0.9566	0.8581
O	0.6680	0.0456	0.1090
O	0.6680	0.0456	0.6090
O	0.3338	0.5446	0.3922
O	0.3338	0.5446	0.8922
O	0.1646	0.4551	0.1423
O	0.1645	0.4551	0.6423

**Table S7.** All the relaxed atomic coordinates used in the simulation of LiFePO<sub>4</sub>.

	x	y	z
Li	1.0000	1.0000	1.0000
Li	0.5000	1.0000	0.5000
Li	0.5000	0.5000	0.5000
Li	0.0000	0.5000	0.0000
Fe	0.2804	0.2500	0.9759
Fe	0.2196	0.7500	0.4759
Fe	0.7804	0.2500	0.5241
Fe	0.7196	0.7500	0.0241
P	0.0943	0.2500	0.4194
P	0.4057	0.7500	0.9194
P	0.5943	0.2500	0.0806
P	0.9057	0.7500	0.5806
O	0.0955	0.2500	0.7460
O	0.4045	0.7500	0.2460
O	0.5955	0.2500	0.7540
O	0.9045	0.7500	0.2540
O	0.4552	0.2500	0.2081
O	0.0448	0.7500	0.7081
O	0.9552	0.2500	0.2919
O	0.5448	0.7500	0.7919
O	0.1663	0.0451	0.2851
O	0.3337	0.9549	0.7851
O	0.6663	0.4549	0.2149
O	0.8337	0.5451	0.7149
O	0.8337	0.9549	0.7149
O	0.6663	0.0451	0.2149
O	0.3337	0.5451	0.7851
O	0.1663	0.4549	0.2851

## References

1. D. Vaknin, J. Zarestky, L. Miller, J.-P. Rivera and H. Schmid, *Phys. Rev. B*, 2002, **65**, 224414.
2. J. B. Goodenough, *Phys. Rev.*, 1968, **171**, 466-479.
3. J. Okamoto, H. Nakao, Y. Yamasaki, H. Wadati, A. Tanaka, M. Kubota, K. Horigane, Y. Murakami and K. Yamada, *J. Phys. Soc. Jpn.*, 2014, **83**, 044705.
4. M. S. a. I. S. Suzuki, *Department of Physics, State University of New York at Binghamton.*
5. A. Osnis, M. Kosa, D. Aurbach and D. T. Major, *J. Phys. Chem. C*, 2013, **117**, 17919-17926.
6. K. Yamauchi, T. Oguchi and S. Picozzi, *J. Phys. Soc. Jpn.*, 2014, **83**, 094712.
7. N. V. Kosova, O. A. Podgornova, E. T. Devyatkina, V. R. Podugolnikov and S. A. Petrov, *Journal of Materials Chemistry A*, 2014, DOI: 10.1039/C4TA04221B.
8. W. Tian, J. Li, J. W. Lynn, J. L. Zarestky and D. Vaknin, *Phys. Rev. B*, 2008, **78**, 184429.
9. J. Li, V. O. Garlea, J. L. Zarestky and D. Vaknin, *Phys. Rev. B*, 2006, **73**, 024410.
10. D. Dai, M. H. Whangbo, H. J. Koo, X. Rocquefelte, S. Jobic and A. Villesuzanne, *Inorg. Chem.*, 2005, **44**, 2407-2413.